

## Paleomagnetism and U–Pb geochronology of the Black Range dykes, Pilbara Craton, Western Australia: a Neoproterozoic crossing of the polar circle

D. A. D. Evans <sup>a</sup>, A.V. Smirnov <sup>b</sup> and A. P. Gumsley <sup>c</sup>

<sup>a</sup>Department of Geology & Geophysics, Yale University, New Haven, CT 06520-8109, USA; <sup>b</sup>Department of Geological & Mining Engineering & Sciences, Michigan Technological University, Houghton, MI 49931-1295, USA; <sup>c</sup>Department of Geology, Lund University, Lund 223 62, Sweden

### ABSTRACT

We report a new paleomagnetic pole for the Black Range Dolerite Suite of dykes, Pilbara craton, Western Australia. We replicate previous paleomagnetic results from the Black Range Dyke itself, but find that its magnetic remanence direction lies at the margin of a distribution of nine dyke mean directions. We also report two new minimum ID-TIMS  $^{207}\text{Pb}/^{206}\text{Pb}$  baddeleyite ages from the swarm, one from the Black Range Dyke itself ( $>2769 \pm 1$  Ma) and another from a parallel dyke whose remanence direction lies near the centre of the dataset ( $>2764 \pm 3$  Ma). Both ages are slightly younger than a previous combined SHRIMP  $^{207}\text{Pb}/^{206}\text{Pb}$  baddeleyite weighted mean date from the same swarm, with slight discordance interpreted as being caused by thin metamorphic zircon overgrowths. The updated Black Range suite mean remanence direction ( $D = 031.5^\circ$ ,  $I = 78.7^\circ$ ,  $k = 40$ ,  $\alpha_{95} = 8.3^\circ$ ) corresponds to a paleomagnetic pole calculated from the mean of nine virtual geomagnetic poles at  $03.8^\circ\text{S}$ ,  $130.4^\circ\text{E}$ ,  $K = 13$  and  $A_{95} = 15.0^\circ$ . The pole's reliability is bolstered by a positive inverse baked-contact test on a younger Round Hummock dyke, a tentatively positive phreatomagmatic conglomerate test, and dissimilarity to all younger paleomagnetic poles from the Pilbara region and contiguous portions of Australia. The Black Range pole is distinct from that of the Mt Roe Basalt (or so-called 'Package 1' of the Fortescue Group), which had previously been correlated with the Black Range dykes based on regional stratigraphy and imprecise SHRIMP U–Pb ages. We suggest that the Mt Roe Basalt is penecontemporaneous to the Black Range dykes, but with a slight age difference resolvable by paleomagnetic directions through a time of rapid drift of the Pilbara craton across the Neoproterozoic polar circle.

### ARTICLE HISTORY

Received 10 December 2016  
Accepted 29 January 2017

### KEYWORDS

paleomagnetism; U–Pb geochronology; Black Range Dolerite Suite; Pilbara craton; Western Australia; Neoproterozoic

### Introduction

Precambrian craton reconstructions require high-quality paleomagnetic poles from well-dated and well-preserved rocks. The question of whether Earth's supercontinent cycle began in Archean or Proterozoic time (Bleeker, 2003; Evans, 2013; Van Kranendonk & Kirkland, 2016) hinges on identifying former 'supercontinent' connections and assessing whether those connections amalgamated into a single Neoproterozoic supercontinent, named Kenorland (Williams, Hoffman, Lewry, Monger, & Rivers, 1991), or whether instead they were embedded within continent-sized blocks (Bleeker, 2003). One classic supercontinent is Vaalbara, the hypothesised conjunction of Kaapvaal craton, in southern Africa, with the Pilbara craton in Western Australia (Cheney, 1996). Different alternative reconstruction models (ibid., de Kock, Evans, & Beukes, 2009; Zegers, de Wit, Dann, & White, 1998) place the two cratons adjacent to each other in various relative locations and orientations.

The constituent cratons of Vaalbara have yielded a uniquely comprehensive dataset of Archean paleomagnetic directions, owing to their equally unique preservation of low-grade volcano-sedimentary rocks. On the Pilbara, initial

success in obtaining coherent remanence directions from Fortescue lavas (Irving & Green, 1958) inspired further investigations of those rocks with similar results (Schmidt & Embleton, 1985). The most recent published paleomagnetic study documented Earth's oldest recorded stratabound magnetic reversal and quantified cratonic drift velocities comparable with those of the last few hundred million years (Strik, Blake, Zegers, White, & Langereis, 2003). Further data also led to a revised reconstruction of Vaalbara that demarcates a simple pattern of depositional facies across the supercontinent, in conjunction with paleomagnetic studies (de Kock *et al.*, 2009).

Pre-Fortescue basement in the Pilbara craton has good potential for extending the paleomagnetic record before ca 2770 Ma, in order to determine whether geodynamo records and tests of plate velocities can be extended back further into Archean time (e.g. Bradley, Weiss, & Buick, 2015). The purpose of the present study is to begin such efforts by refining the Black Range suite of dykes paleomagnetic pole, using paleomagnetism integrated with U–Pb baddeleyite geochronology. Our results have important implications for stratigraphic correlations in the north-central Pilbara region.

## Stratigraphic context

Archean stratigraphy of the Pilbara craton can be divided into two temporally and structurally defined successions (Figure 1). The older succession generally has granitoid–greenstone dome–trough crustal architecture with ages between *ca* 3500 and 2800 Ma, and is divided into the Pilbara and De Grey Supergroups in the East Pilbara Terrane or their lateral equivalents in the West Pilbara Terrane (Hickman, 2012; Van Kranendonk *et al.*, 2006a). Following a large-scale regional unconformity, the second succession begins with the volcanic-dominated Fortescue Group and related intrusions within the time interval *ca* 2800–2700 Ma (Thorne & Trendall, 2001), followed conformably by the largely sedimentary Hamersley Group that extends into Paleoproterozoic time (Trendall, 1983). The Fortescue–Hamersley succession has been interpreted to record a plate-tectonic evolution from rifting to development of a passive margin (Blake, 1993; Thorne & Trendall, 2001), perhaps initially with the aid of a mantle plume (Arndt, Bruzák, & Reischmann, 2001; Rainbird & Ernst, 2001).

Fortescue Group strata are variable across the craton (Figure 1), but generally include a lowest mafic volcanic unit (Mount Roe Basalt), followed by a sandstone-dominated interval (Hardey Formation), more dominantly mafic volcanic units (variable names), and an uppermost shale-dominated unit (Jeerinah Formation). Felsic igneous rocks (Bamboo Creek and

Spinaway porphyries) locally occur within or adjacent to the Hardey Formation. Around the northern part of the craton, variability can be observed along strike from the west near the Roebourne/Pyramid area, to the east near the Nullagine region and beyond to the Gregory Range. Near the centre of the northern outcrop belt, where the metamorphic grade is lowest (Smith, Perdrix, & Parks, 1982), the Marble Bar Subbasin (an erosional outlier) exposes several alternations of basaltic lava and siliciclastic sedimentary rock that are disconnected from other Fortescue Group exposures. In that region, the stratigraphically lowest package was moderately to steeply folded prior to deposition of the overlying succession (Blake, 1993).

The Mount Roe Basalt, referred to as Fortescue Group 'Package 1' in the sequence-stratigraphic framework of Blake (1993) and Blake, Buick, Brown, and Barley (2004), has been dated by U–Pb methods in three localities:  $2763 \pm 13$  Ma (SHRIMP on zircon) near the type locality at Roebourne (Arndt, Nelson, Compston, Trendall, & Thorne, 1991),  $2775 \pm 10$  Ma (SHRIMP on zircon) in the far southwest area of the craton (*ibid.*), and  $2767 \pm 3$  (TIMS on air-abraded zircon;  $\sim 1.4\%$  discordant) in an isolated exposure near the southern edge of the Marble Bar outlier (Van Kranendonk, Bleeker, & Ketchum, 2006b). Ages from the overlying Hardey Formation interval include a volcanic member in the easternmost Pilbara ( $2764 \pm 8$  Ma, SHRIMP on zircon; Arndt *et al.*, 1991); two

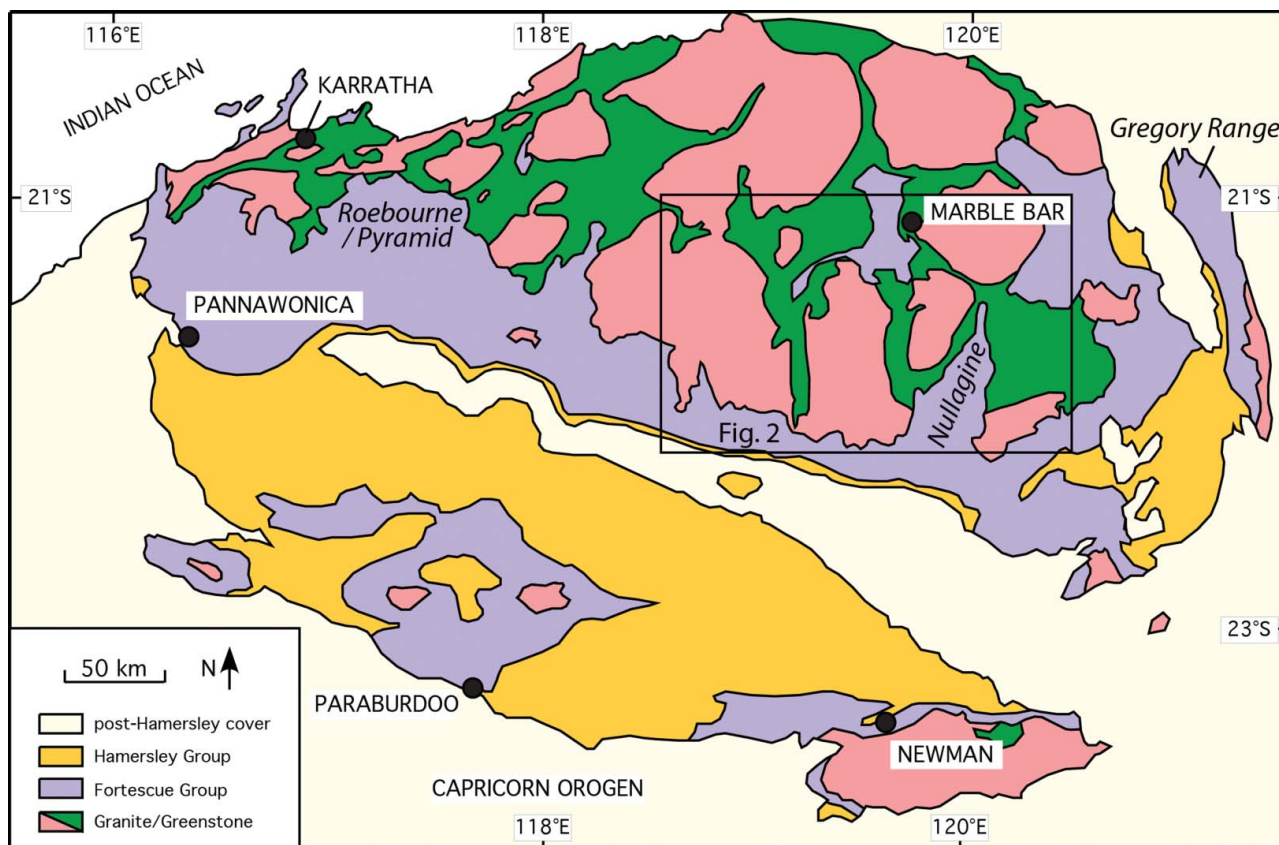
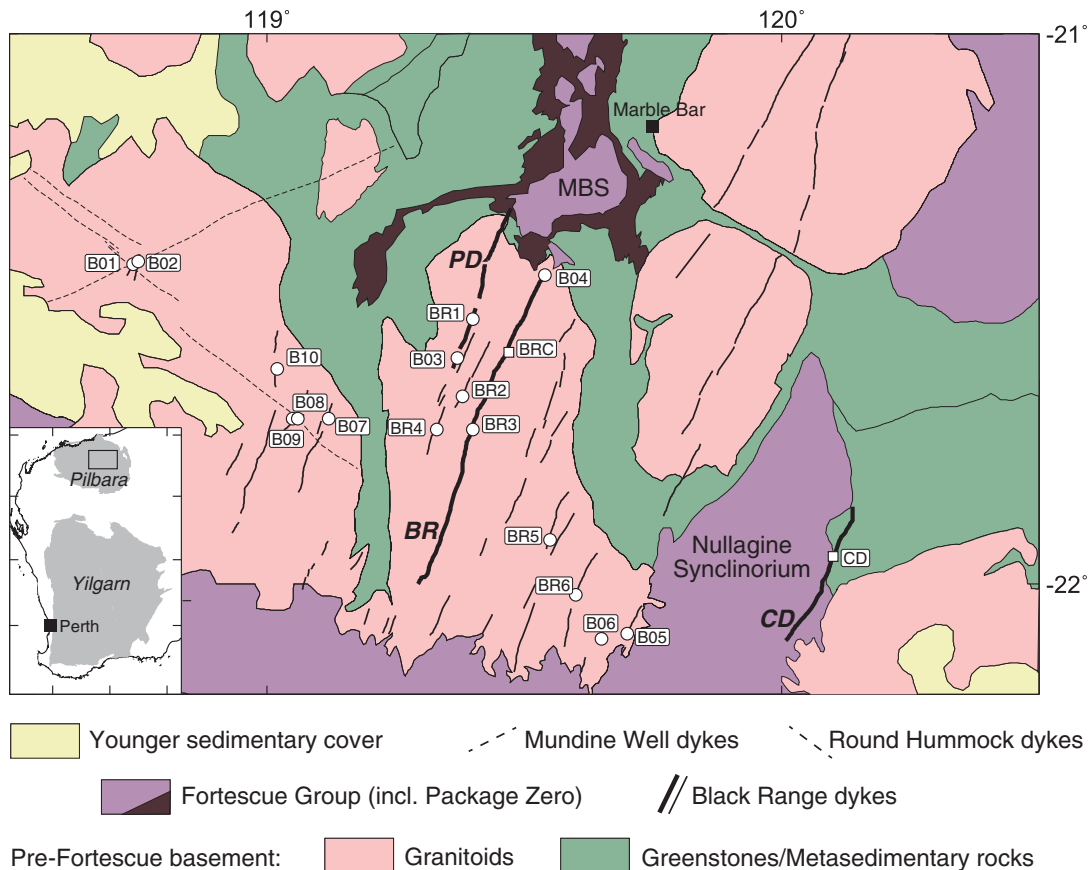


Figure 1. Simplified map of the Pilbara cratonic region, showing the sampling area relative to other exposures of Fortescue Group and related intrusive rocks.

porphyries in east-central part of the craton, Spinaway ( $2768 \pm 16$  Ma conventional U–Pb on zircon, Pidgeon, 1984;  $2766 \pm 2$  Ma, SHRIMP U–Pb on zircon, Blake *et al.*, 2004) and Bamboo Creek ( $2756 \pm 8$  Ma, SHRIMP on zircon; Arndt *et al.*, 1991); a lower rhyolite unit ( $2766 \pm 3$  Ma; Blake *et al.*, 2004); a felsic tuff near the top of the sequence ( $2752 \pm 5$  Ma; Blake *et al.*, 2004); and a volcanic unit within the sandstone in the southern region ( $2750 \pm 5$  Ma; Hall, 2005). The latter three ages were all obtained by U–Pb SHRIMP methods on zircon.

For many years, it has been considered that eruption of the Mount Roe Basalt was coincident with emplacement of the Black Range Dolerite Suite of NNE-trending mafic dykes, which include both the Black Range Dyke itself and the Cajuput Dyke farther to the east (Figure 2)—the latter of which is nonconformably overlain by Hardey Formation sandstone (Hickman, 1983; Lewis, Rosman, & de Laeter, 1975). The correlation of Mount Roe Basalt and the Black Range dyke swarm was strengthened by an integrated  $^{207}\text{Pb}$ – $^{206}\text{Pb}$  SHRIMP baddeleyite age of  $2772 \pm 2$  Ma for the dykes (Wingate, 1999), which was within uncertainty of the previous Mount Roe Basalt ages (Arndt *et al.*, 1991). The Black Range and Cajuput dykes also share a paleomagnetic remanence direction (Embleton, 1978) with that of the Mount Roe Basalt (Schmidt & Embleton, 1985; Strik *et al.*, 2003), thus appearing to reinforce the correlation even further.

Nonetheless, near the southwestern edge of the Marble Bar Sub-basin (Figure 2), at least one dyke of the Black Range suite (herein referred to as the Pilga dyke, with new U–Pb geochronology presented below) intrudes the lowermost lava package—moderately tilted as noted above, and shown on published Geological Survey of Western Australia (GSWA) quadrangle maps as Mount Roe Basalt (Hickman, 2010, 2013; Hickman & Lipple, 1978; Van Kranendonk, 2000). What might be a northward, right-stepping en echelon offset of that dyke also appears to intrude lavas correlated with the Kylena basalt, which would be surprising, as the Kylena Formation (in its type locality) is definitively younger than Hardey Formation sandstone and has yielded ages in the range of *ca* 2760–2740 Ma (Blake *et al.*, 2004). Such stratigraphic relationships prompted Van Kranendonk (2000) to conclude that the Pilga dyke ‘must belong to a younger set.’ Not all Fortescue stratigraphers agree, however, with the mapped correlations by GSWA in the Marble Bar Sub-basin. Blake (1993) maintained correlation of the lowest Marble Bar Sub-basin basalt package, which attains steep dips, with the subhorizontal Mount Roe Basalt of the Nullagine area, but correlated the overlying, subhorizontal lavas of his ‘Glen Herring Creek Sequence’ to the Hardey Formation rather than Kylena Formation (Figure 3). With further modification, Strik (2004) discovered that the lowest Marble Bar Sub-basin lava succession (with locally



**Figure 2.** Location of sampling sites (circles, this study; squares, Embleton, 1978) and simplified geology of the sampling area. The Black Range Dolerite Suite of mafic dykes includes the Pilga dyke (PD), Black Range Dyke (BR) and Cajuput Dyke (CD). MBS, Marble Bar Sub-basin. Inset map shows the location of our sampling area within the Pilbara cratonic area (box) in Western Australia.

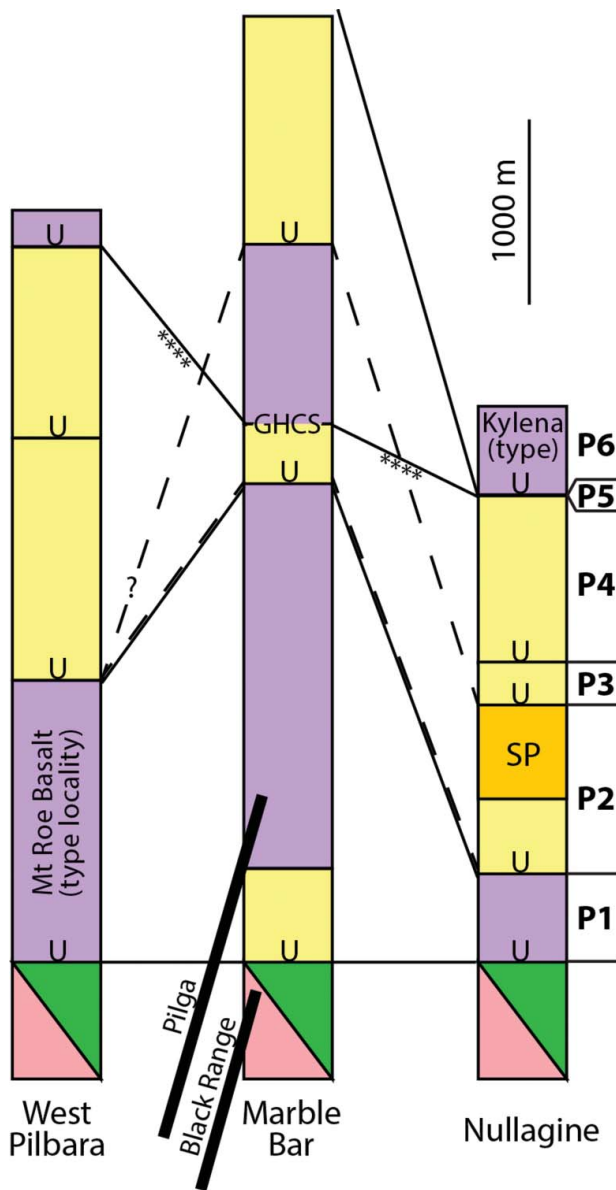


Figure 3. Alternative published stratigraphic correlations across the northern Pilbara craton, as of 2003, modified after Blake (1984). Unconformities are denoted by 'U.' Dashed lines: correlations of Blake (1984). Undecorated solid lines: correlations of Blake (1993) including GHCS, Glen Herring Creek Sequence. Solid lines marked with '\*\*\*\*' are correlations from published editions of the Marble Bar geological maps at 1:250 000 scale (Hickman, 2010, 2013; Hickman & Lipple, 1978) and 1:100 000 scale (Hickman & Van Kranendonk, 2008). Nullagine synclinorium stratigraphic sequence 'packages' P1–P6 follow Blake *et al.* (2004); the stratigraphy continues higher than shown. SP, Spinaway felsic porphyry of Lipple (1975), included within the Bamboo Creek Member of the Hardy Formation by Thorne and Trendall (2001) and Hickman (2007).

steep dips) has a distinct paleomagnetic remanence from Mount Roe Basalt in other regions of the northern Pilbara. According to paleomagnetic correlations by Strik (2004), the lowest lavas in the Marble Bar Sub-basin were named 'Package 0,' and the overlying Glen Herring Creek Sequence lavas would more appropriately correlate to 'Package 1' of the Mount Roe Basalt (Strik *et al.*, 2003). These alternative correlations could allow the entire Black Range suite of dykes, including the Pilga dyke, to occupy a single stratigraphic position

consistent with available geochronology: penecontemporaneous to 'Package 1.'

The present paper describes new geochronological and paleomagnetic data from the Black Range dyke swarm, and discusses how the new data can be interpreted in a new, integrated litho- and chronostratigraphy for the northern Pilbara region in Neoproterozoic times.

## Methods

Geochronological processing was made at the Department of Geology in Lund University, where dolerite dyke sample C09B03 (Pilga dyke) and C08BR3 (Black Range Dyke at Hillside) were crushed and milled in order to extract baddeleyite. Extraction was carried out using the water-based separation technique of Söderlund and Johansson (2002) with a Wilfley Table. The best-quality baddeleyite crystals were hand-picked and combined into fractions comprising between one to five crystals each, and placed in separate pre-cleaned Teflon capsules in a fume hood within the clean laboratory at Lund University. The baddeleyite grain fractions in the capsules were then washed thoroughly in steps with small quantities of ultrapure HNO<sub>3</sub> and H<sub>2</sub>O. After washing the Teflon capsules containing the cleaned baddeleyite grains, a spike solution consisting of <sup>205</sup>Pb, <sup>233</sup>U and <sup>236</sup>U was added to every capsule together with concentrated ultrapure HF. The capsules were then placed in an oven at 200°C for three days in order to dissolve the baddeleyite grains and homogenise the initial and spike U and Pb solutions together. In the clean laboratory at the Department of Geosciences in the Museum of Natural History (Stockholm), the Teflon capsules containing the sample solutions were then placed on a hot plate at 100°C until the combined solution evaporated in a fume hood. Ultrapure 6 M HCl and 0.25 M H<sub>3</sub>PO<sub>4</sub> was then added to each capsule before being dried down once again on the hot-plate at 100°C, leaving a small sample droplet. These droplets in the capsules consist of the dissolved sample fraction and spike in H<sub>3</sub>PO<sub>4</sub> that was then further redissolved in 2 µL of Si-gel prepared using a recipe of Gerstenberger and Haase (1997) before being loaded on outgassed Re filaments.

The analyses were made on the Finnigan Triton mass spectrometer at the Department of Geosciences, Swedish Museum of Natural History in Stockholm following the same procedure as that employed by Gumsley *et al.* (2015). The Re filaments with the samples were loaded onto a carousel and mounted, and then heated, in the high vacuum chamber in the mass spectrometer. The Pb isotopes were measured after being heated and emitted in a temperature range of approximately 1210–1250°C. The isotopes <sup>204</sup>Pb, <sup>205</sup>Pb, <sup>206</sup>Pb, <sup>207</sup>Pb and <sup>208</sup>Pb were measured in either static mode with Faraday detectors, or in peak-switching mode with a Secondary Electron Multiplier amplifier. Age, size and quantity of grains could be linked to whether static or peak-switching mode was used. Large samples with high <sup>206</sup>Pb/<sup>205</sup>Pb ratios and strong and stable signals were preferentially measured in static mode. Upon completion of the Pb isotopic analyses, the filament temperatures were increased to

Table 1. ID-TIMS baddeleyite isotopic data from the Pilga and Black Range dykes.

Analysis no. (no. of grains)	U/Th	P <sub>bc</sub> /Pb <sub>tot</sub> raw <sup>b</sup>	<sup>206</sup> Pb/ <sup>204</sup> Pb	<sup>207</sup> Pb/ <sup>235</sup> U (corr.) <sup>c</sup>	± 2σ % error	<sup>206</sup> Pb/ <sup>238</sup> U	± 2σ % error	<sup>207</sup> Pb/ <sup>235</sup> U (age, Ma)	<sup>206</sup> Pb/ <sup>238</sup> U	<sup>207</sup> Pb/ <sup>206</sup> Pb	± 2σ	Concordance (%)
<b>Pilga (C09B03): 2763.9 ± 3.3 Ma, 1/6 point <sup>207</sup>Pb/<sup>206</sup>Pb minimum date</b>												
a (4)	4.6	0.015	3905.0	13.965	0.337	0.527	0.314	2747.3	2728.0	2761.6	2.2	98.8
b (3)	3.0	0.021	2770.9	13.826	0.568	0.524	0.553	2737.9	2716.8	2753.5	3.5	98.7
c (5)	9.0	0.054	1175.8	13.988	0.845	0.527	0.844	2748.9	2728.5	2763.9	3.4	98.7
d (1)	15.5	0.093	693.5	14.185	1.458	0.536	1.459	2762.1	2766.8	2758.7	5.7	100.3
e (2)	2.2	0.047	1337.5	13.971	0.745	0.528	0.739	2747.7	2735.1	2757.0	3.2	99.2
f (4)	4.6	0.034	1771.7	13.554	0.589	0.515	0.570	2719.0	2678.9	2749.1	3.3	97.4
<b>Black Range (C08BR3): 2769.4 ± 1.0 Ma, 1/5 point <sup>207</sup>Pb/<sup>206</sup>Pb minimum date</b>												
a (1)	43.6	0.019	3223.1	12.451	0.453	0.488	0.448	2639.0	2563.9	2697.2	1.6	95.1
b (1)	74.4	0.042	1476.7	13.374	0.905	0.506	0.888	2706.4	2640.7	2755.9	3.9	95.8
c (1)	43.1	0.010	6281.7	13.981	0.217	0.527	0.202	2748.4	2730.3	2761.8	1.4	98.9
d (1)	52.5	0.057	1092.7	14.085	1.068	0.532	1.057	2755.4	2748.8	2760.3	4.4	99.6
e (1)	49.4	0.005	11955.1	14.185	0.242	0.533	0.236	2762.1	2752.3	2769.4	1.0	99.4

<sup>a</sup>P<sub>bc</sub> = common Pb; Pb<sub>tot</sub> = total Pb (radiogenic + blank + initial). <sup>b</sup> Measured ratio, corrected for mass fractionation and spike. <sup>c</sup> Isotopic ratios corrected for mass fractionation (0.1‰ per amu for Pb, determined by replicate analyses of NBS standard SRM. 981 and SRM 983), spike contribution (<sup>205</sup>Pb–<sup>233</sup>U–<sup>236</sup>U tracer solution), blank (1 pg Pb and <0.1 pg U), and initial common Pb. Initial common Pb corrected with isotopic compositions from the model of Stacey and Kramers (1975) at the age of the sample. corr. = corrected

between 1310–1320°C, where <sup>235</sup>U and <sup>238</sup>U isotopes were emitted and measured. An ‘in-house’ program made by Per-Olof Persson (Department of Geosciences, Natural History Museum, Stockholm) with calculations following Ludwig (2001) was used for data handling, and final age calculations were made using Isoplot (Ludwig, 2001).

For paleomagnetic studies, we sampled 16 sites representing 14 separate dykes in the northeastern part of the Pilbara craton (Figure 2). Seven to 17 field-drilled, oriented, 2.5 cm-diameter core samples were collected from each site. Orientation was done with both solar and magnetic compasses. Although outcrops were screened with a compass for notable magnetic deflections by lightning, at some sites minor deflections were unavoidable owing to limited outcrop.

Magnetic remanence measurements were conducted at Michigan Technological University using an automated three-axis DC-SQUID 2G rock magnetometer housed in a magnetically shielded room. After measurement of the natural remanent magnetisation (NRM), the samples were cycled through the Verwey transition at ~120 K (Verwey, 1939) by immersing them into liquid nitrogen for about 2 h in order to reduce a viscous component carried by larger magnetite grains (Schmidt, 1993). The low-temperature treatment was followed by 15–20 thermal demagnetisation steps performed in an inert (nitrogen) atmosphere. Progressive demagnetisation was carried out until the magnetic intensity of the samples dropped below system noise level or until the measured directions became erratic and unstable (typically at 580–590°C).

The characteristic remanent magnetisation (ChRM) for samples displaying near-linear demagnetisation trajectories was isolated using principal-component analysis (Kirschvink, 1980). The best-fit line was used if defined by at least five consecutive demagnetisation steps that trended toward the origin and had a maximum angle of deviation less than 10°. The mean directions were calculated using Fisher statistics (Fisher, 1953). A site mean was accepted for further calculations if it was obtained from three or more samples, and the confidence circle radius ( $\alpha_{95}$ ) was smaller than 10°.

## Results and discussion

### Geochronology

Both mafic dyke samples yielded abundant fragments of euhedral baddeleyite with thin surface coatings, frosty in appearance, which are interpreted as zircon overgrowths (cf. Heaman & LeCheminant, 1993). Such overgrowths are well documented in mafic rocks of high metamorphic grade, but the north-central Pilbara has experienced only prehnite–pumpellyite metamorphism (Smith *et al.*, 1982), dated by monazite at ca 2160 Ma (Rasmussen, Fletcher, & Sheppard, 2005). If zirconium mobilisation during that episode (or some other secondary event) caused the minor zircon overgrowth, then each analysis would measure a mixture of the primary baddeleyite cores, and a small contribution from secondary zircon rims, and thus underestimate the age of baddeleyite crystallisation. Our choices for calculating the data of the subsets (Table 1) are made with these factors under consideration.

From the Pilga sample C09B03 (Figure 4), six fractions were analysed, each combining between one and five grains. Fraction (d) was the only single-grain baddeleyite analysed. <sup>207</sup>Pb/<sup>206</sup>Pb dates from the six analyses ranged between 2764 Ma and 2749 Ma, with concordance varying from 97% to 100%. The oldest <sup>207</sup>Pb/<sup>206</sup>Pb date of 2763.9 ± 3.4 Ma (fraction c), at 99% concordance, is interpreted to provide a minimum age for the Pilga dyke emplacement.

From the Black Range Dyke sample C08BR3, five single grains were analysed. Two grains (fractions a, b), had variable concordance between 95 and 96% (Figure 4) and are not considered further. Fractions (c, d, e), however, were between 99 and 100% concordant and yielded variable <sup>207</sup>Pb/<sup>206</sup>Pb dates between 2769 Ma and 2760 Ma. As such, the oldest <sup>207</sup>Pb/<sup>206</sup>Pb date of 2769.4 ± 1.0 Ma on fraction (e) likely represents the best minimum estimate for the age of baddeleyite crystallisation.

These new two <sup>207</sup>Pb/<sup>206</sup>Pb TIMS ages are comparable with the previously published weighted mean <sup>207</sup>Pb/<sup>206</sup>Pb SHRIMP baddeleyite age of 2772 ± 2 Ma for the Black Range Dolerite Suite (Wingate, 1999), as shown in Figure 4b. The oldest TIMS analysis on our Black Range sample (fraction e) has a

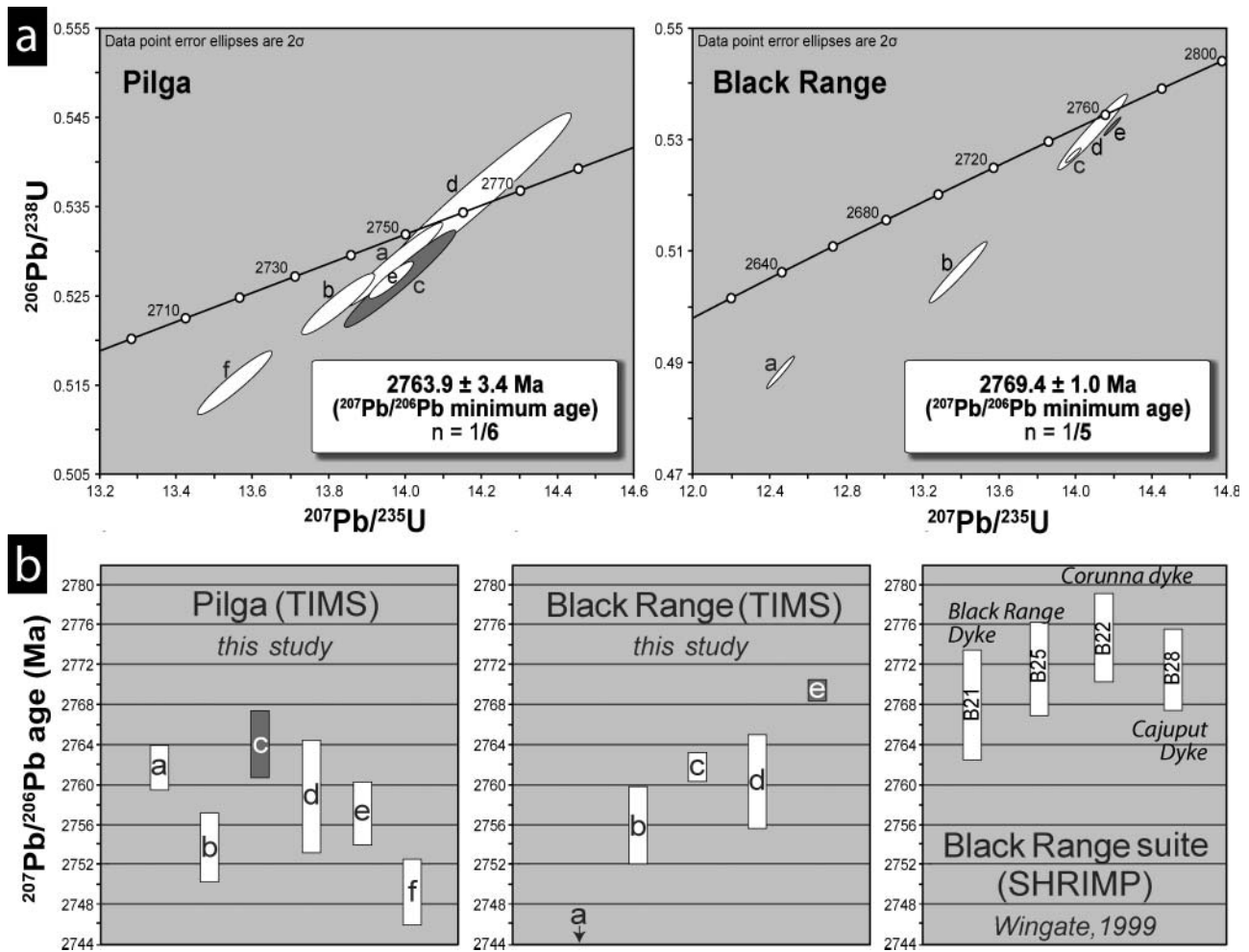


Figure 4. (a) Wetherill U–Pb ID-TIMS concordia diagrams for the analysed baddeleyite from the Pilga and Black Range dykes, with the error ellipses demarcating individual fractions analysed, for details see Table 1. (b)  $^{207}\text{Pb}/^{206}\text{Pb}$  plots of the individual baddeleyite fractions analysed in this study for the Pilga and Black Range dykes at left, with a comparison of complete  $^{207}\text{Pb}/^{206}\text{Pb}$  ages by SHRIMP also shown of the Black Range Dolerite Suite by Wingate (1999) at right, which were combined into the  $2772 \pm 2$  Ma mean age in that study.

$^{207}\text{Pb}/^{206}\text{Pb}$  age within error of the mean SHRIMP result from the same dyke and suggests that our preferred method of selecting the oldest-age fraction is the most accurate assessment of the variable TIMS data, at least in this instance. SHRIMP analyses on the interior domains of baddeleyite grains are better placed to avoid zircon overgrowths and generate unbiased ages of crystallisation, despite being less precise.

Interpretation of the Pilga dyke data is hindered by the absence of a SHRIMP result on the same intrusion as a reference. The preferred  $2764 \pm 3$  Ma result provides a minimum date for dyke emplacement, but it remains unclear whether the Pilga and Black Range dykes are strictly coeval, or whether the Pilga dyke could have intruded several million years after the other dykes in the Black Range suite. Regardless, the Pilga data are clearly more similar to the SHRIMP results from the Mount Roe Basalt, rather than the Kylene Formation, with implications for Fortescue Group correlations between Marble Bar Sub-basin and other outcrop areas.

### Paleomagnetism

Most sites exhibited one or two components of remanent magnetisation (Figure 5). Most samples showed a consistent high unblocking temperature ( $\sim 500$ – $580^\circ\text{C}$ ) ChRM with steep downward directions, generally N to E in declination. Low-moderate-temperature components were generally scattered or had a weak tendency toward low inclinations to the WNW or ENE; in only two sites were such overprints coherent enough to produce a clustered mean direction (site BR4,  $D = 299^\circ$ ,  $I = 10^\circ$ ,  $\alpha_{95} = 8^\circ$ ,  $N = 6/7$ ; and site B05,  $D = 305^\circ$ ,  $I = -35^\circ$ ,  $\alpha_{95} = 10^\circ$ ,  $N = 8/12$ ), which could possibly date from the regional low-grade metamorphic event at  $ca$  2160 Ma (Rasmussen *et al.*, 2005). Exceptions to these general trends were observed in samples with anomalously high values of NRM intensity and parallel components removed by both liquid nitrogen treatment and moderate levels (300– $500^\circ\text{C}$ ) of thermal demagnetisation. We strongly suspect such sites to be affected by lightning; some sites with consistent and anomalous moderate-temperature components (e.g. BR1,

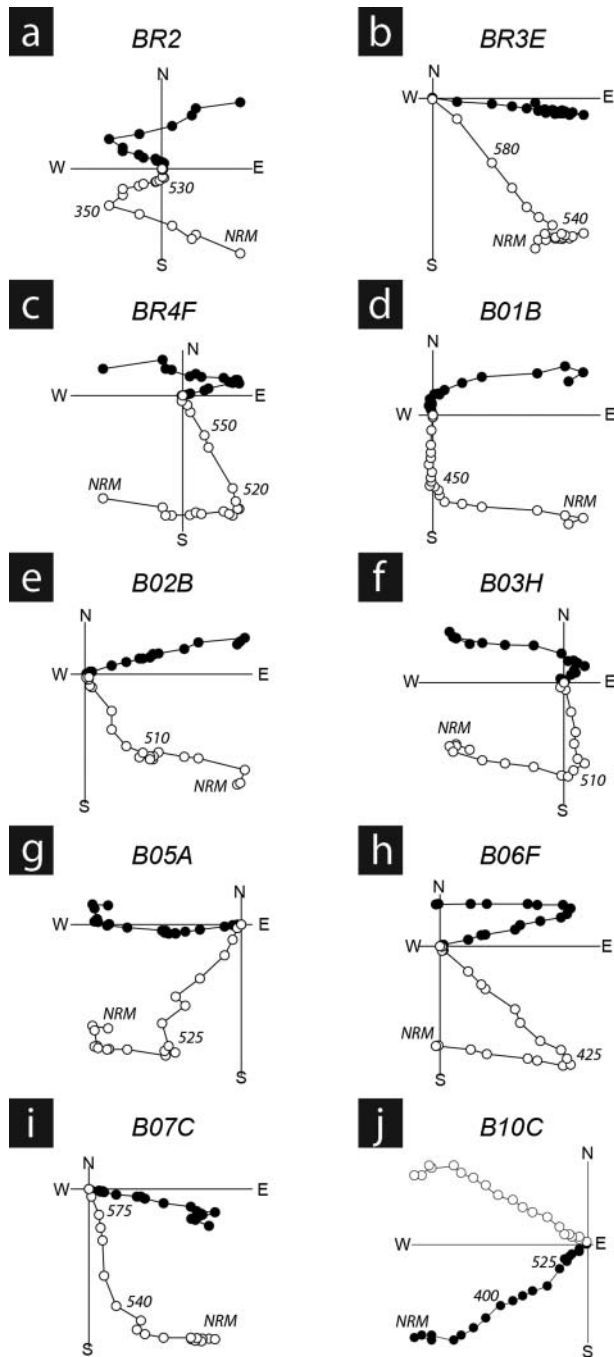


Figure 5. Typical orthogonal vector plots of thermal demagnetisation (vertical/horizontal projections shown by open/filled symbols) from the Black Range dykes. Panels (a–i) show sites used to calculate the grand mean; panel (j) shows an anomalous site that was excluded (Table 2). Numbers indicate temperature steps (in °C).

BR5) are interpreted to represent the distal tangential magnetic field about the point of lightning impact. The other two sites with coherent, non-modal ChRM directions (BR6, B10; both toward the SW but with opposing signs of inclination) did not have the same demagnetisation behaviour as the modal sites: rather than sharp unblocking spectra restricted to  $>500^{\circ}\text{C}$ , those two sites' ChRM vectors had distributed unblocking through  $\sim 250\text{--}570^{\circ}\text{C}$  (Figure 5j). The origin of

their remanence vectors is uncertain, but they are clearly anomalous relative to the Black Range suite as a whole (Table 2).

Figure 6 summarises data from each of the nine sites that are included in the mean Black Range suite paleomagnetic direction. We replicate the SE-down ChRM direction for the Black Range Dyke itself at the Hillside locality (Embleton, 1978), but we find that such a direction lies, together with that of the Cajuput Dyke (ibid.) and its easterly satellite dyke (Strik *et al.*, 2003), at the outer edge of the modal distribution of NE-down remanence directions (Figure 7). We attribute the differences in remanence of the various Black Range suite dykes to paleosecular variation of the Neoproterozoic geodynamo. An alternative interpretation might be that the Black Range and Cajuput dykes are older than other dykes in the swarm; the Pilga and other dykes bearing the mean NE-down ChRM could be a few million years younger as allowed by our new  $^{207}\text{Pb}/^{206}\text{Pb}$  age constraints (Figure 4). That model, however, would require a complex pattern of ChRM oscillations in stratigraphic sequence: from NW-down of Package 0 (Strik, 2004), to SE-down of the Black Range and Cajuput dykes (Embleton, 1978; this study), to NE-down of the Pilga and other dykes (this study), and back to SE-down in the higher Fortescue basalt packages (Schmidt & Embleton, 1985; Strik *et al.*, 2003). We prefer the simpler model of a single age for the Black Range Dolerite Suite, with its NE-down ChRM falling neatly between those of Package 0 and Package 1 basalts (Strik, 2004). In local coordinates, the mean Black Range suite direction (Table 2) is parameterised by  $D = 031.5^{\circ}$ ,  $I = 78.7^{\circ}$ ,  $k = 40$ , and  $\alpha_{95} = 8.3^{\circ}$ , and the corresponding paleomagnetic pole, calculated from the mean of nine virtual geomagnetic poles, is at  $03.8^{\circ}\text{S}$ ,  $130.4^{\circ}\text{E}$ ,  $K = 13$ , and  $A_{95} = 15.0^{\circ}$ .

Reliability of our new Black Range dykes pole is affirmed by an inverse baked-contact test with a Round Hummock dyke in the western part of our study area, near Obstinate Creek. Site C09B02, from a N- to NNE-striking dyke, yields a steep NE-downward ChRM typical of the Black Range suite. About 1.5 km to the south, the same Black Range dyke is cross-cut by a NW-striking dyke of the Round Hummock swarm (site I09R4). In that locality, the younger Round Hummock dyke carries a NW-down remanence direction (Figure 8) that is typical for the Round Hummock swarm, which has a preliminary ID-TIMS U–Pb baddeleyite date of *ca* 1070 Ma (D. Evans and A. Gumsley, unpublished; details to be presented in a forthcoming manuscript). The Black Range dyke samples from that site, all within 5 m of the Round Hummock dyke, carry a ChRM at moderate unblocking temperatures between  $300\text{--}375^{\circ}\text{C}$ , likely held by contact-metamorphic pyrrhotite generated at the time of Round Hummock intrusion. Although the baked Black Range dyke remanence is likely a crystallisation-remnant magnetisation rather than a thermal-remnant magnetisation, effects from the time of Round Hummock intrusion are clearly apparent. For the purposes of the present contribution, this positive inverse baked-contact test demonstrates that the Black Range suite characteristic remanence is older than *ca* 1070 Ma. A second baked-contact test was attempted at site C09B08, where a member of the Black Range suite is

Table 2. Summary of ChRM results from the Black Range dykes.

Site ID	$\lambda_s$ (°S)	$\Phi_s$ (°E)	$N$	$B$	$D$ (°)	$I$ (°)	$k$	$\alpha_{95}$ (°)	$\lambda_p$ (°N)	$\Phi_p$ (°E)	$K$	$A_{95}$ (°)
C08 BR1 <sup>a</sup> ('Pilga dyke')	21.520	119.400	7		174.1	18.2		15.5	–	–		
C08 BR2	21.662	119.381	7	✓	038.5	65.5		8.9	12.5	144.8		
C08 BR3 Black Range Dyke	21.720	119.404	7	✓	099.5	77.9		6.2	–23.6	144.3		
C08 BR4	21.716	119.334	7	✓	059.2	78.7		2.7	–09.6	138.2		
C08 BR5 <sup>a</sup>	21.923	119.549	7		004.6	00.8		8.6	–	–		
C08 BR6 <sup>a</sup>	22.015	119.603	8		236.0	50.4		8.0	–	–		
C09 B01	21.421	118.743	7	✓	005.8	73.0		3.3	09.9	121.8		
C09 B02	21.415	118.748	6	✓	045.2	71.8		3.2	03.2	141.7		
B02 baked by I09R4 <sup>a</sup>	21.429	118.747	12		341.8	51.9		4.2	–	–		
I09R4 <sup>a</sup> (Round Hummock)	21.429	118.747	4		308.2	52.2		4.7	–	–		
C09 B03 'Pilga dyke'	21.585	119.370	10	✓	033.9	75.1		4.3	02.2	134.6		
C09 B04 <sup>a,b</sup>	21.441	119.541	6		287.4	–30.1		79.5	–	–		
C09 B05	22.086	119.703	9	✓	314.9	82.6		7.7	–11.5	109.2		
C09 B06	22.096	119.645	7	✓	348.6	65.1		8.0	20.0	111.4		
C09 B07	21.699	119.118	8	✓	161.6	81.2		3.0	–37.9	125.9		
C09 B08 baked by I09R5 <sup>a</sup>	21.703	119.065	7		323.4	68.7		1.5	–	–		
I09R5 <sup>a</sup> (Round Hummock dyke)	21.703	119.065	12		332.8	47.5		3.3	–	–		
C09 B09 <sup>a,c</sup>	21.703	119.065	–		–	–		–	–	–		
C09 B10 <sup>a</sup>	21.606	119.020	8		245.5	–25.6		15.3	–	–		
Black Range Dyke at Hillside <sup>a,d,e</sup>	21.72	119.40	9		093.0	76.0		8.0	–	–		
Black Range Dyke at Cooglegong Creek <sup>a,d</sup>	21.58	119.47	7		131.2	64.8		4.5	–	–		
Cajuput Dyke <sup>a,d</sup>	21.95	120.10	9		145.0	71.0		13	–47.6	149.0		
<b>Total mean—This study only</b>				<b>9</b>	<b>31.5</b>	<b>78.7</b>	<b>40</b>	<b>8.3</b>	<b>–3.8</b>	<b>130.4</b>	<b>13</b>	<b>15.0</b>

<sup>a</sup>Site is not used for calculation of the mean direction. <sup>b</sup> Conglomerate/breccia test. <sup>c</sup> Significantly scattered within-site directions. <sup>d</sup> Data from Embleton (1978). <sup>e</sup> Equivalent to Site C08BR3.

$\lambda_s$ ,  $\Phi_s$  are the site latitude and longitude.  $N$  is the number of samples used to calculate the paleomagnetic declination ( $D$ ) and inclination ( $I$ );  $\alpha_{95}$  and  $k$  are the 95% confidence circle and the concentration parameter for paleomagnetic directions.  $B$  is the number of sites used for a between-site mean direction.  $\lambda_p$  and  $\Phi_p$  are the latitude and longitude of the virtual geomagnetic pole (VGP).  $A_{95}$  and  $K$  are the 95% confidence circle and the concentration parameter for VGP distribution.

intruded by another Round Hummock dyke, which is 23 m wide at the intersection. Round Hummock dyke samples there (site I09R5) yield a typical NW-moderate-down ChRM direction from that swarm, but Black Range dyke rocks within 2 m of the contact have a steeper NW-down direction that is intermediate between the Round Hummock remanence and other

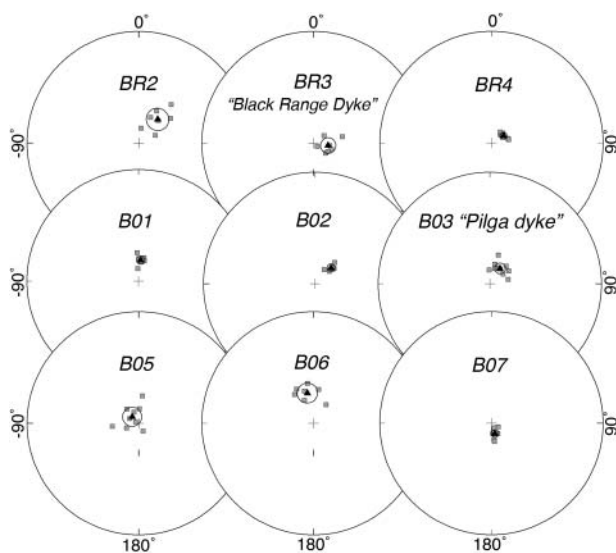


Figure 6. Site-mean paleomagnetic remanence directions from the Black Range dykes used to calculate the mean (Table 2). Equal-area plots show the accepted paleomagnetic directions (grey squares) and their means (solid triangle) with the 95% confidence circle ( $\alpha_{95}$ ) for each site.

Black Range directions (Table 2). As no more distant rocks were sampled from that particular Black Range intrusion, the test remains inconclusive.

As a final attempted test on the age of Black Range dykes' remanence, fine-grained mafic pebbles ('basalt droplets') in the granite boulder volcanic conglomerate unit of Van Kranendonk *et al.* (2006b) were individually sampled from a locality within a few hectometres of the exposed tip of the Black Range Dyke. Low-temperature components are generally directed north and upward, parallel to Earth's present magnetic field at the sampling site (Figure 9a); some samples exhibited only this presumably recent component. Other samples, collected from one side of the outcrop, show a univectorial, west-horizontal magnetisation that unblocks at temperatures generally below 500°C (Figure 9b); that direction is dissimilar to all previously documented paleomagnetic results from the northern Pilbara cratonic region and must represent a very localised overprint of unknown age. Among clasts located at the other side of the outcrop, six out of eight specimens carry a distinct ChRM after removal of the low-temperature present-field component; these higher-temperature directions, retaining stability as demagnetisation end-points from about 500 to 540°C, are quite dispersed (labelled 'SEP' in Figure 9c). The six stable end-point (SEP) vectors have a resultant mean length of 3.01; a test for uniformity against a unimodal alternative (Fisher, Lewis, & Embleton, 1987, p. 110) indicates that a uniform ('random') distribution on the sphere cannot be rejected at the 95% confidence level, a positive statistical test. The unblocking temperatures from the suite of

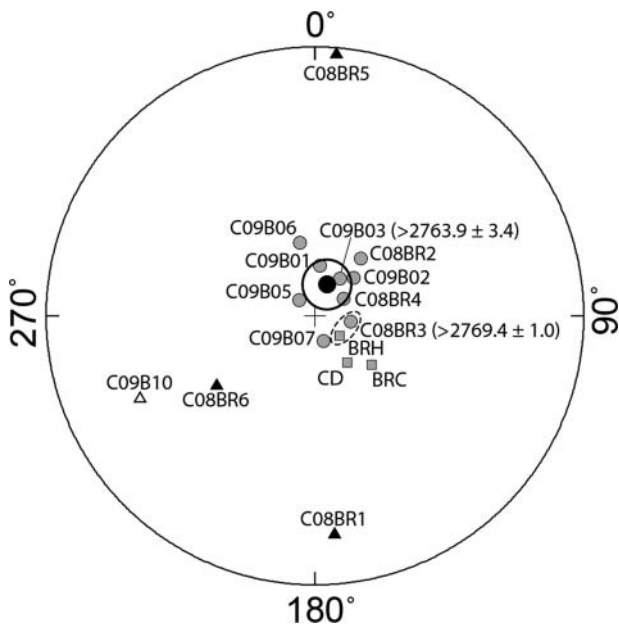


Figure 7. Summary of paleomagnetic results from the Black Range dykes. Grey circles show the accepted directions from this study; grey squares show the site-means from Embleton (1978); BRC, Black Range Dyke at Cooglegong Creek; BRH, Black Range Dyke at Hillside; CD, Cajuput Dyke (Table 1). Dashed ellipse encloses the data from Hillside locality of the Black Range Dyke, sampled by both Embleton (1978) and this study. Solid circle is the grand mean calculated from this study, with associated cone of 95% confidence (Table 2). Upright triangles show the Black Range Suite site-means from this study that are not used in the mean calculation.

'basalt droplet' clasts, however, are lower than either Black Range dykes (this study) or Mount Roe Basalt (Strik, 2004; Strik *et al.*, 2003), so the test must be considered only tentatively positive. The data are consistent with a low-temperature phreatomagmatic recrystallisation or solid-state remagnetisation of the basalt droplets prior to their incorporation into the conglomerate, which was formed penecontemporaneously to the Black Range Dyke intrusion (Van Kranendonk *et al.*, 2006b). Most definitively, the steep NE-down mean ChRM observed in the Black Range Dolerite Suite is not observed as a consistent overprint at the conglomerate site. The Shipunov, Muraviev, and Bazhenov (1998) test on that Black Range mean direction and the six conglomerate clast end-points also indicates consistency of their being drawn from a uniform ('random') distribution at the 95% confidence level.

In addition to the field tests described above, including the positive inverse baked-contact test at Obstinate Creek, an additional consideration on the age of the Black Range suite mean magnetic remanence, is the fact that its pole is distinct from all younger poles derived from Western Australia, and also all Precambrian poles generated in rocks of the North Australian craton after the latter has been restored to the West+South Australian reference frame according to Li and Evans (2011). There is broad similarity of our new Black Range suite pole to that of the first paleomagnetic analysis on the Ediacaran–Cambrian Arumbera Sandstone in central Australia (Embleton,

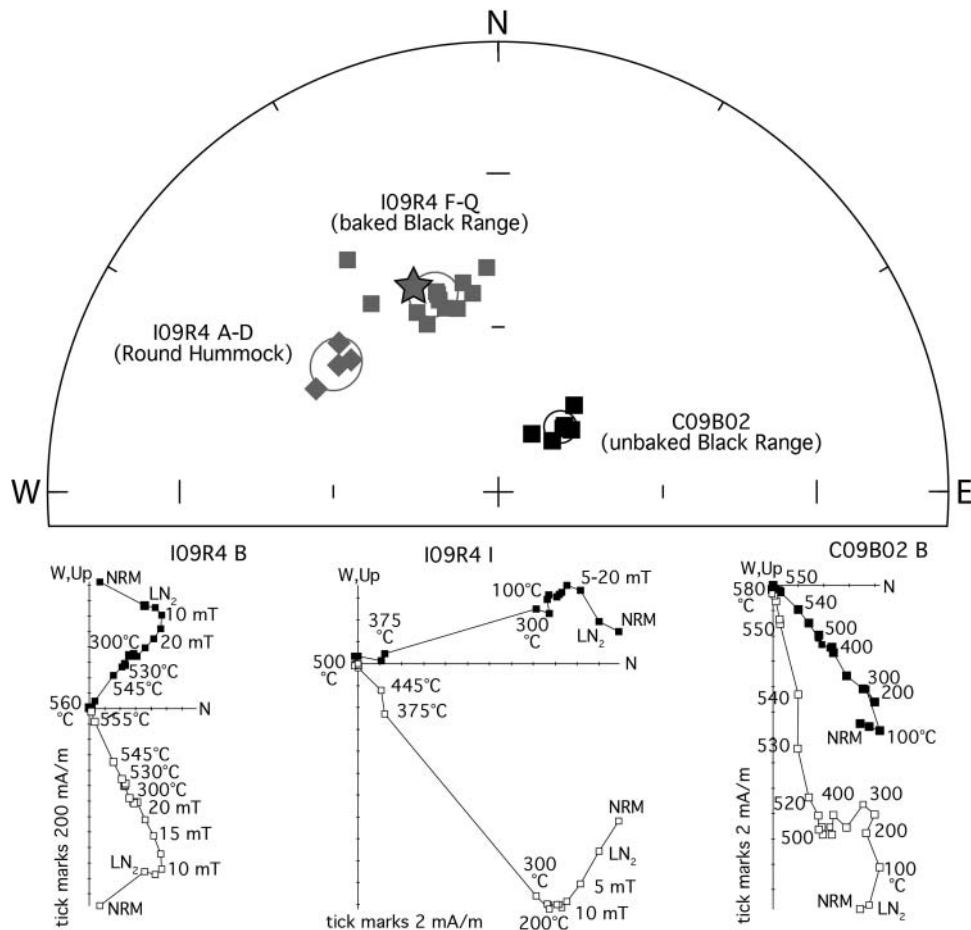
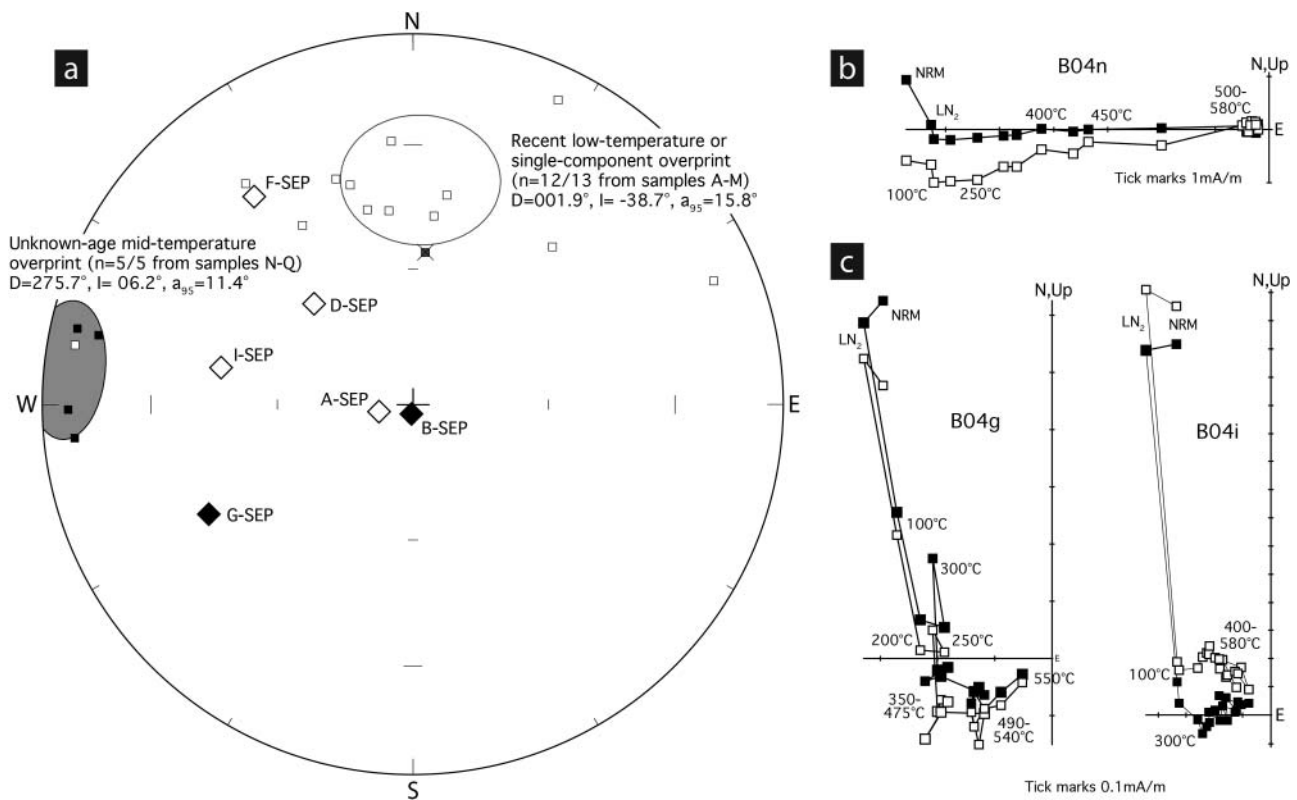


Figure 8. Inverse baked-contact test of a Black Range suite dyke (C09B02) intruded by a ca 1070 Ma Round Hummock dyke (I09R4) near Obstinate Creek in the western part of the study area. All stereonet vector end-points are in the lower hemisphere; squares, Black Range dyke; diamonds, Round Hummock dyke; star, expected magnetic direction from the Warakurna large igneous province mean pole (Wingate, Pisarevsky, & Evans, 2002). Orthogonal projection symbols as in Figure 5.



**Figure 9.** Phreatomagmatic breccia test from the tip of the Black Range Dyke. (a) Equal-area projection of vector component directions. Squares, low- and mid-temperature components of magnetisation; diamonds, stable end-point (SEP) vectors from samples in the outcrop area less affected by the localised mid-temperature overprint. (b) Orthogonal projection diagram of a sample with a mid-temperature overprint. (c) Orthogonal projection diagrams of samples with both low- and high-temperature components.

1972). However, that younger direction is likely a mid-Carboniferous overprint related to the Alice Springs Orogeny (Li, Powell, & Thrupp, 1990), and Paleozoic overprinting of the Black Range suite is precluded by our field stability tests. To summarise the quality of the new Black Range suite pole: on the seven-point reliability scale (Q) of Van der Voo (1990), it scores six out of seven points, lacking only dual polarity of the remanence. That criterion is met, however, by the Nullagine succession in the same region (Strik *et al.*, 2003; Table 3).

Our new paleomagnetic pole for the Black Range dyke suite (Figure 10) lies midway between poles from two unconformity-bounded sequences in the lowermost Fortescue

Group: the informally named Package 1, which is generally correlated with the Mount Roe Basalt (Strik *et al.*, 2003), and the stratigraphically lower Package 0 (Strik, 2004) that is restricted to the Marble Bar Sub-basin and also generally mapped as Mount Roe Basalt (e.g. Hickman, 2010, 2013). Because ages from the rocks mapped as Mount Roe Basalt are either imprecise (Arndt *et al.*, 1991) or of uncertain correlation to the type locality (Van Kranendonk *et al.*, 2006b), the progression of paleomagnetic poles among the Mount Roe Basalt and related units may provide an independent chronometer for magmatism and sedimentation across the northern Pilbara. The poles (Table 3) sweep across the craton in rough

**Table 3.** Late Archean (ca 2800–2700 Ma) paleomagnetic poles from Pilbara craton, Western Australia.

Paleomagnetic pole	Code	Age (Ma)	Method	Pole ( $^\circ$ N, $^\circ$ E)	$A_{95}$ ( $^\circ$ )	1234567 (Q)	Test	References
Fortescue Package 0	P0	$>2772 \pm 2$	SHRIMP-b	-01, 093	8	0111101 (5)	F	Strik, 2004; Wingate, 1999
Black Range suite	BRS	$2772 \pm 2$	SHRIMP-b	-04, 130	15	1111101 (6)	c, G	Wingate, 1999; this study
Fortescue Package 1	P1	ca 2770	(Strat, APW)	-41, 160	4	1111100 (5)	G, M	Strik <i>et al.</i> , 2003; Van Kranendonk <i>et al.</i> , 2006b
Fortescue Package 2	P2	$2766 \pm 2$	SHRIMP-z	-47, 153	15	1011100 (4)	G, M	Blake <i>et al.</i> , 2004; Strik <i>et al.</i> , 2003
Mt Jope volcanics pre-fold	MJV	$>2750 \pm 5$	SHRIMP-z	-41, 129	20	1011100 (4)	f	Hall, 2005; Schmidt & Embleton, 1985
Fortescue Package 4–7	P4–7	ca 2730	SHRIMP-z	-50, 138	13	1110100 (4)	M	Blake <i>et al.</i> , 2004; Strik <i>et al.</i> , 2003
Fortescue Package 8–10	P8–10	ca 2715	SHRIMP-z	-59, 186	6	1110100 (4)	M	Blake <i>et al.</i> , 2004; Strik <i>et al.</i> , 2003
Southern Hamersley VH	SVH	$2717 \pm 2$	SHRIMP-z	-65, 204	12	1010100 (3)	–	Blake <i>et al.</i> , 2004; Sumita, Hatakeyama, Yoshihara, & Hamano, 2001

Code, abbreviation shown in Figure 10. (Strat, APW), age estimate from stratigraphic correlation and simple interpolation along a paleomagnetic apparent polar wander path.  $A_{95}$ , Fisher's (1953) confidence cone radius. Q, reliability from Van der Voo (1990). The fourth criterion of a field stability test, if positive, is abbreviated as follows: c, inverse baked-contact test; F, intrasuccessional fold test; f, tectonic fold test; G, intrasuccessional conglomerate test; M, magnetostratigraphy test of stratabound reversals in sequence. In these abbreviations, upper-case symbols indicate primary paleomagnetic remanence; lower-case symbols indicate ancient remanence that might be primary but not demonstrated conclusively by the test.

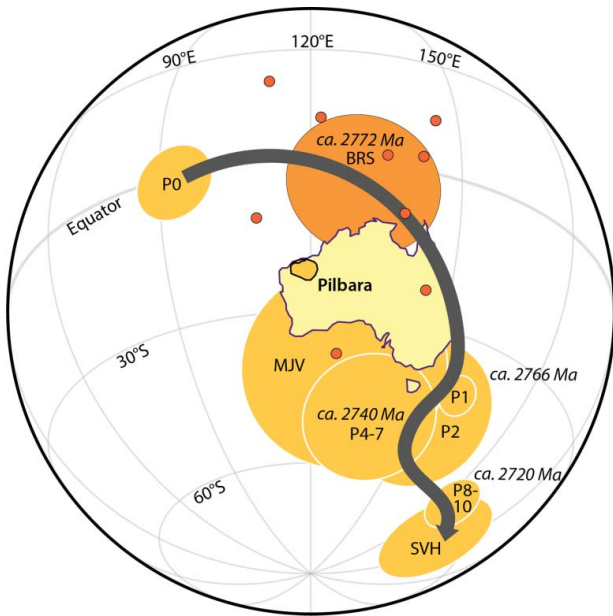


Figure 10. Apparent polar wander path for Pilbara craton during Fortescue Group deposition. Pole abbreviations given in Table 3. Darker shading denotes the mean Black Range suite (BRS) pole and its nine-constituent site-mean virtual geomagnetic poles.

stratigraphic order from NW to SE, and in the absence of a more complex oscillatory apparent polar wander (as in the alternative model of variable Black Range suite ages discussed above), the ages of remanence acquisition should decrease monotonically in that direction. The most parsimonious interpretation of apparent polar wander progression begins with Package 0 sedimentation and basaltic volcanism being restricted to the Marble Bar Sub-basin, followed by folding of that sequence, then intrusion of the Black Range dykes at ca 2772 Ma, and followed further by deposition of the Package 1 sequence and younger clastic and volcanic strata across a much larger area of the craton. During that succession of events, the Pilbara craton crossed polar areas of Earth’s surface. Although Strik (2004) expressed concern about the tectonic feasibility of an approximately 180° change in magnetic remanence declination between Package 0 and Package 1, such a shift in declination naturally arises from simple translation by a rigid tectonic block across the geographic pole.

The above model of a simple polar crossing at ca 2772 Ma generates specific correlations of unconformity-bounded sequences in the lower Fortescue Group, especially in the Marble Bar Sub-basin (Figure 11). The correlations adopted herein are identical to those suggested by Strik (2004) and would require revision to geological quadrangle maps published by the GSWA (e.g. Hickman, 2010, 2013; Hickman & Van Kranendonk, 2008). On those maps that include the Marble Bar Sub-basin, the ‘Kylena Formation’ (correlated paleomagnetically to Package 1 of Strik *et al.*, 2003) would need to be reassigned to the Mount Roe Basalt. If new lithostratigraphic designations for the immediately underlying ‘Hardey Formation’ sandstone unit and lower Package 0 lavas are desired, then local names

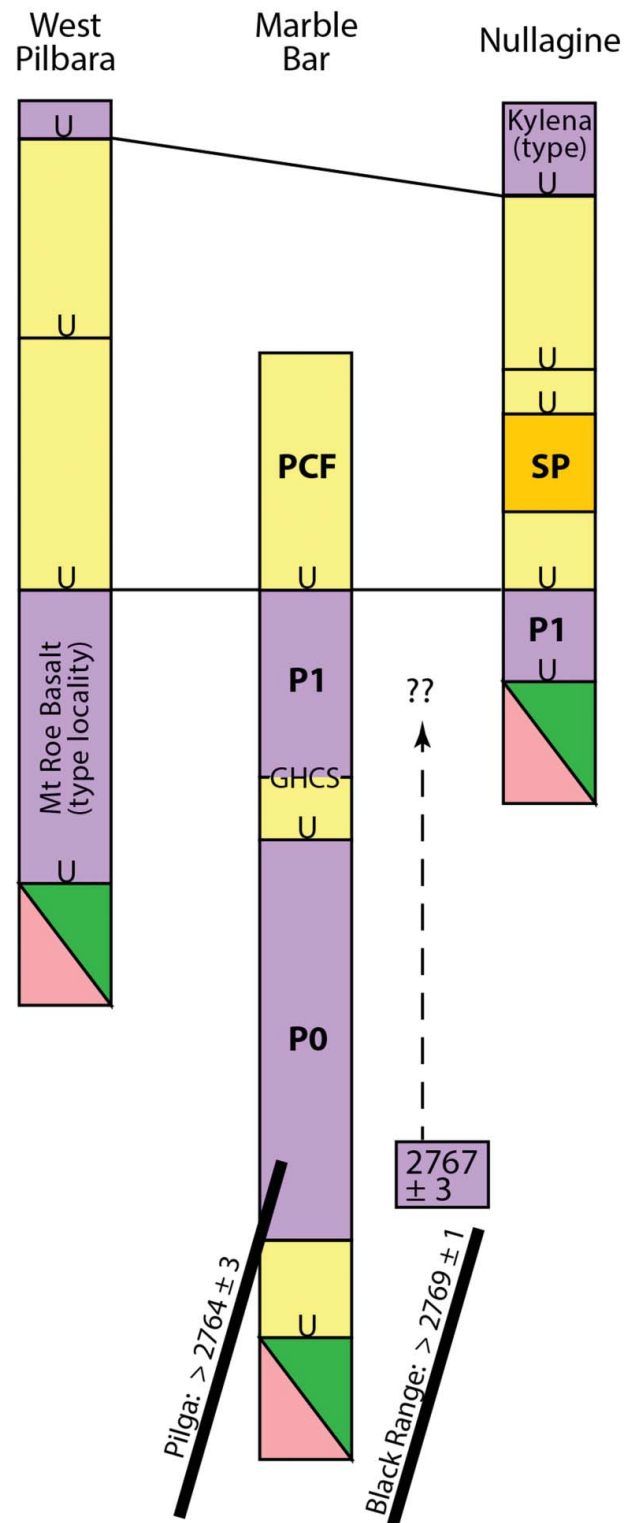


Figure 11. Revised correlations of lower Fortescue Group strata across northern Pilbara craton, according to paleomagnetic and ID-TIMS <sup>207</sup>Pb/<sup>206</sup>Pb geochronologic data. Abbreviations as in Figure 3, plus the following: P0, Package 0 of Strik (2004); PCF, Pear Creek Formation.

from the Marble Bar Sub-basin would need to replace ‘Mount Roe Basalt’ as currently mapped in that area. The U–Pb TIMS age of 2767 ± 3 Ma from an isolated outcrop of shallowly dipping strata near the tip of the Black Range

Dyke (Van Kranendonk *et al.*, 2006b) could reasonably apply to either of the two lowest volcanic packages of the Fortescue Group, although paleomagnetic analysis on those particular-dated strata could help resolve the issue. At stratigraphically higher levels, the conglomeratic 'Pear Creek Formation' could retain its unique name in the Marble Bar Sub-basin, or it might eventually be incorporated within the Hardey Formation if age constraints permit. As summarised above, the Spinaway porphyry lies within sedimentary rocks of the Hardey Formation in the Nullagine region and has been dated by U–Pb SHRIMP on zircon at  $2766 \pm 2$  Ma (Blake *et al.*, 2004). Our preferred correlations are consistent with that date and younger ages from the Fortescue Group (*ibid.*).

## Conclusions

The present study has produced a revised, high-quality paleomagnetic pole from the Black Range suite of mafic dykes, constrained by minimum  $^{207}\text{Pb}$ – $^{206}\text{Pb}$  ages on baddeleyite from two intrusions at  $2769 \pm 1$  Ma (the Black Range Dyke itself) and  $2764 \pm 3$  Ma (the Pilga dyke). The best estimate for the crystallisation age of the Black Range Dolerite Suite remains  $2772 \pm 2$  from an earlier study (Wingate, 1999), but our data include the Pilga dyke as a likely member of that swarm—contrary to earlier suggestions. The new paleomagnetic data indicate a polar crossing by the Pilbara craton during initial development of rifting and volcanism as manifested by lowermost strata in the Fortescue Group. New correlations of those strata indicate that rifting began in the localised region of the Marble Bar Sub-basin and was followed by Black Range suite dyke emplacement at  $2772 \pm 2$  Ma and subsequent development of craton-wide magmatism and sedimentation.

## Acknowledgements

We thank D. Chad Moore, Ian Rose and Taylor Kilian for field assistance; Martin Van Kranendonk for logistical advice; and Jennifer Kasbohm, Blair Schoene and Michael Wingate for discussions during preparation of the manuscript. Michael Wingate and Sergei Pisarevsky are also thanked for their constructive reviews of the manuscript. Funding was provided by the U.S. National Science Foundation, Swedish Research Council, Royal Physiographic Society in Lund, and Yale University.

## Disclosure statement

No potential conflict of interest was reported by the authors.

## ORCID

D. A. D. Evans  <http://orcid.org/0000-0001-8952-5273>  
A. P. Gumsley  <http://orcid.org/0000-0003-1395-3065>

## References

- Arndt, N. T., Bruzak, G., & Reischmann, T. (2001). The oldest continental and oceanic plateaus: Geochemistry of basalts and komatiites of the Pilbara Craton, Australia. In R. E. Ernst & K. L. Buchan (Eds.), *Mantle plumes: Their identification through time* (pp. 359–387). 359–387. Boulder, Co: Geological Society of America Special Paper, 352.
- Arndt, N. T., Nelson, D. R., Compston, W., Trendall, A. F., & Thorne, A. M. (1991). The age of the Fortescue Group, Hamersley Basin, Western Australia, from ion microprobe zircon U–Pb results. *Australian Journal of Earth Sciences*, 38, 261–281.
- Blake, T. S. (1984). Evidence for stabilization of the Pilbara Block, Australia. *Nature*, 307, 721–723.
- Blake, T. S. (1993). Late Archaean crustal extension, sedimentary basin formation, flood basalt volcanism and continental rifting: The Nullagine and Mount Jope Supersequences, Western Australia. *Precambrian Research*, 60, 185–241.
- Blake, T. S., Buick, R., Brown, S. J. A., & Barley, M. E. (2004). Geochronology of a Late Archaean flood basalt province in the Pilbara Craton, Australia: Constraints on basin evolution, volcanic and sedimentary accumulation, and continental drift rates. *Precambrian Research*, 133, 143–173.
- Bleeker, W. (2003). The late Archean record: A puzzle in ca. 35 pieces. *Lithos*, 71, 99–134.
- Bradley, K., Weiss, B. P., & Buick, R. (2015). Records of geomagnetism, climate, and tectonics across a Paleoproterozoic erosion surface. *Earth and Planetary Science Letters*, 419, 1–13.
- Cheney, E. S. (1996). Sequence stratigraphy and plate tectonic significance of the Transvaal succession of southern Africa and its equivalent in Western Australia. *Precambrian Research*, 79, 3–24.
- de Kock, M. O., Evans, D. A. D., & Beukes, N. J. (2009). Validating the existence of Vaalbara in the Neoarchean. *Precambrian Research*, 174, 145–154.
- Embleton, B. J. J. (1972). The palaeomagnetism of some Proterozoic–Cambrian sediments from the Amadeus Basin, central Australia. *Earth and Planetary Science Letters*, 17, 217–226.
- Embleton, B. J. J. (1978). The palaeomagnetism of 2400 m.y. old rocks from the Australian Pilbara craton and its relation to Archaean–Proterozoic tectonics. *Precambrian Research*, 6, 275–291.
- Evans, D. A. D. (2013). Reconstructing pre-Pangean supercontinents. *Geological Society of America Bulletin*, 125, 1735–1751.
- Fisher, R. A. (1953). Dispersion on a sphere. *Proceedings Royal Society A*, 217, 295–305.
- Fisher, N. I., Lewis, T., & Embleton, B. J. J. (1987). *Statistical analysis of spherical data*. Cambridge, UK: Cambridge University Press, 313 pp.
- Gerstenberger, H., & Haase, G. (1997). A highly effective emitter substance for mass spectrometric Pb isotope ratio determinations. *Chemical Geology*, 136, 309–312.
- Gumsley, A., Olsson, J., Söderlund, U., de Kock, M., Hofmann, A., & Klausen, M. (2015). Precise U–Pb baddeleyite age dating of the Usushwana Complex, southern Africa—Implications for the Mesoarchaean magmatic and sedimentological evolution of the Pongola Supergroup, Kaapvaal Craton. *Precambrian Research*, 267, 174–185.
- Hall, C. E. (2005). SHRIMP U–Pb depositional age for the lower Hardey Formation: Evidence for diachronous deposition of the lower Fortescue Group in the southern Pilbara region, Western Australia. *Australian Journal of Earth Sciences*, 52, 403–410.
- Heaman, L. M., & LeCheminant, A. N. (1993). Paragenesis and U–Pb systematics of baddeleyite (ZrO<sub>2</sub>). *Chemical Geology*, 110, 95–126.
- Hickman, A. H. (1983). *Geology of the Pilbara Block and its environs*. Western Australia Geological Survey, Bulletin 127, Perth, WA: Western Australia Geological Survey, 268 p.
- Hickman, A. H. (compiler) (2007). Nullagine. *Western Australia Geological Survey 1:250 000 Geological Map Sheet SF 51-05* (3rd ed.). Perth, WA: Western Australia Geological Survey.
- Hickman, A. H. (compiler) (2010). Marble Bar. *Western Australia Geological Survey 1:250 000 Geological Map Sheet SF 50-8* (3rd ed.). Perth, WA: Western Australia Geological Survey.
- Hickman, A. H. (2012). Review of the Pilbara Craton and Fortescue Basin, Western Australia: Crustal evolution providing environments for early life. *Island Arc*, 21, 1–31.
- Hickman, A. H. (compiler) (2013). North Shaw. *Western Australia Geological Survey 1:100 000 Geological Map Sheet 2755* (2nd ed.). Perth, WA: Western Australia Geological Survey.

- Hickman, A. H., & Lipple, S. L. (1978). Marble Bar. *Western Australia Geological Survey 1:250 000 Geological Series Explanatory Notes*. Perth, WA: Western Australia Geological Survey, 24 pp.
- Hickman, A. H., & Van Kranendonk, M. V. (compilers) (2008). Marble Bar. *Western Australia Geological Survey 1:100 000 Geological Map Sheet 2855* (1st ed.). Perth, WA: Western Australia Geological Survey.
- Irving, E., & Green, R. (1958). Polar movement relative to Australia. *Geophysical Journal of the Royal Astronomical Society*, 1, 64–72.
- Kirschvink, J. L. (1980). The least squares line and plane and the analysis of paleomagnetic data. *Geophysical Journal of the Royal Astronomical Society*, 62, 699–718.
- Lewis, J. D., Rosman, K. J. R., & de Laeter, J. R. (1975). The age and metamorphic effects of the Black Range dolerite dyke. Western Australia Geological Survey, Annual Report for the Year 1974 (pp. 80–88). Perth, WA: Western Australia Geological Survey.
- Li, Z.-X., & Evans, D. A. D. (2011). Late Neoproterozoic 40° intraplate rotation within Australia allows for a tighter-fitting and longer-lasting Rodinia. *Geology*, 39, 39–42.
- Li, Z. X., Powell, C. McA., & Thrupp, G. A. (1990). Australian Palaeozoic palaeomagnetism and tectonics—II. A revised apparent polar wander path and palaeogeography. *Journal of Structural Geology*, 12, 567–575.
- Lipple, S. L. (1975). Definitions of new and revised stratigraphic units of the Eastern Pilbara Region. *Western Australia Geological Survey, Annual Report for the Year 1974* (pp. 58–63). Perth, WA: Western Australia Geological Survey.
- Ludwig, K. R. (2001). Isoplot: A Geochronological Toolkit for Microsoft Excel, Berkeley Geochronology Center, USA, Special Publication No. 1a. Berkeley, Cal: University of California.
- Pidgeon, R. T. (1984). Geochronological constraints on early volcanic evolution of the Pilbara Block, Western Australia. *Australian Journal of Earth Sciences*, 31, 237–242.
- Rainbird, R. H., & Ernst, R. E. (2001). The sedimentary record of mantle-plume uplift. In R. E. Ernst & K. L. Buchan (Eds.), *Mantle plumes: Their identification through time* (pp. 227–245). Boulder, Co: Geological Society of America Special Paper, 352.
- Rasmussen, B., Fletcher, I. R., & Sheppard, S. (2005). Isotopic dating of the migration of a low-grade metamorphic front during orogenesis. *Geology*, 33, 773–776.
- Schmidt, P. W. (1993). Paleomagnetic cleaning strategies. *Physics of the Earth and Planetary Interiors*, 76, 169–178.
- Schmidt, P. W., & Embleton, B. J. J. (1985). Prefolding and overprint magnetic signatures in Precambrian (~2.9–2.7 Ga) igneous rocks from the Pilbara Craton and Hamersley Basin, NW Australia. *Journal of Geophysical Research*, 90, 2967–2984.
- Shipunov, S. V., Muraviev, A. A., & Bazhenov, M. L. (1998). A new conglomerate test in palaeomagnetism. *Geophysical Journal International*, 133, 721–725.
- Smith, R. E., Perdrix, J. L., & Parks, T. C. (1982). Burial metamorphism in the Hamersley Basin, Western Australia. *Journal of Petrology*, 23, 75–102.
- Söderlund, U., & Johansson, L. (2002). A simple way to extract baddeleyite (ZrO<sub>2</sub>). *Geochemistry Geophysics Geosystems*, 3, 1–7.
- Stacey, J. S., & Kramers, J. D. (1975). Approximation of terrestrial lead isotope evolution by a two stage model. *Earth and Planetary Science Letters*, 26, 207–221.
- Strik, G. H. M. A. (2004). *Palaeomagnetism of late Archaean flood basalt terranes: Implications for early Earth geodynamics and geomagnetism* (PhD thesis). Geologica Ultraiectina, Mededelingen van de Faculteit Geowetenschappen Universiteit Utrecht, Utrecht, Netherlands, 242, 160 pp.
- Strik, G., Blake, T. S., Zegers, T. E., White, S. H., & Langereis, C. G. (2003). Palaeomagnetism of flood basalts in the Pilbara Craton, Western Australia: Late Archaean continental drift and the oldest known reversal of the geomagnetic field. *Journal of Geophysical Research*, 108, doi:10.1029/2003JB002475
- Sumita, I., Hatakeyama, T., Yoshihara, A., & Hamano, Y. (2001). Paleomagnetism of late Archean rocks of Hamersley basin, Western Australia and the paleointensity at early Proterozoic. *Physics of the Earth and Planetary Interiors*, 128, 223–241.
- Thorne, A. M., & Trendall, A. F. (2001). *Geology of the Fortescue Group, Pilbara Craton, Western Australia*. Perth, WA: Western Australia Geological Survey, Bulletin, 144, 249 pp.
- Trendall, A. F. (1983). The Hamersley Basin. In A. F. Trendall & R. C. Morris (Eds.), *Iron-formation: Facts and problems* (pp. 69–129). Amsterdam: Elsevier.
- Van der Voo, R. (1990). The reliability of paleomagnetic data. *Tectonophysics*, 184, 1–9.
- Van Kranendonk, M. J. (2000). Geology of the North Shaw 1:100 000 Sheet. Western Australia Geological Survey 1:100 000 Geological Series Explanatory Notes. Perth, WA: Western Australia Geological Survey, 86 pp.
- Van Kranendonk, M. J., Bleeker, W., & Ketchum, J. (2006b). Phreatomagmatic boulder conglomerates at the tip of the ca 2772 Ma Black Range dolerite dyke, Pilbara Craton, Western Australia. *Australian Journal of Earth Sciences*, 53, 617–630.
- Van Kranendonk, M. J., Hickman, A. H., Smithies, R. H., Williams, I. R., Bagas, L., & Farrell, T. R. (2006a). Revised lithostratigraphy of Archean supracrustal and intrusive rocks in the northern Pilbara Craton, Western Australia. *Western Australia Geological Survey, Record*, 2006/15. Perth, WA: Western Australia Geological Survey, 57 pp.
- Van Kranendonk, M. J., & Kirkland, C. L. (2016). Conditioned duality of the Earth system: Geochemical tracing of the supercontinent cycle through Earth history. *Earth-Science Reviews*, 160, 171–187.
- Verwey, E. J. W. (1939). Electronic conduction of magnetite (Fe<sub>3</sub>O<sub>4</sub>) and its transition point at low-temperature. *Nature*, 44, 327–328.
- Williams, H., Hoffman, P. F., Lewry, J. F., Monger, J. W. H., & Rivers, T. (1991). Anatomy of North America: Thematic geologic portrayals of the continent. *Tectonophysics*, 187, 117–134.
- Wingate, M. T. D. (1999). Ion microprobe baddeleyite and zircon ages for Late Archaean mafic dykes of the Pilbara Craton, Western Australia. *Australian Journal of Earth Sciences*, 46, 493–500.
- Wingate, M. T. D., Pisarevsky, S. A., & Evans, D. A. D. (2002). Rodinia connections between Australia and Laurentia: No SWEAT, no AUSWUS? *Terra Nova*, 14, 121–128.
- Zegers, T. E., de Wit, M. J., Dann, J., & White, S. H. (1998). Vaalbara, Earth's oldest assembled continent? A combined structural, geochronological, and palaeomagnetic test. *Terra Nova*, 10, 250–259.